SINGLE-PHASE ELECTRICAL SPRING FUZZY CONTROLLER-BASED ANALYSIS OF ACTIVE AND REACTIVE POWER CONTROL CAPABILITY

[1]Ram Reddy Anugu, [2]Bathula Srikanth, [3]Sd. Umar Sayeed, [4]T V Bhaskar

[1,2,3]Assistant Professor, [4]Student, [1,2,3,4]Department of Electrical and Electronics Engineering , Siddhartha Institute of Engineering and Technology, Hyderabad, India.

ABSTRACT

Building a one-phase electric spring with a fuzzy controller based on active and reactive power control is the primary objective of this project. For so-called electric single-stage springs (ES-2) of the second generation, the paper suggests a straightforward power control system that addresses the shortcomings of the current ES control techniques. The unexpected power generated by the RESs is separated into two halves, one absorbed by the still variable ES-2 and the other injected in the controlled grid, using a straightforward and precise signal manipulation that functions both at steady state and during RSE transient. This control is deemed suitable for the generation of distributed energy, especially in homes. The literature backs up the theoretical background of the suggested fluid control. Its performance is checked initially by simulations. A standard RES application is considered for this reason. An electrical spring system with a 49 rules base controller with a fluid control system is ideal in contrast to the traditional PI controller with a faster response time. The modeling is conducted with graphs depicted regarding time in MATLAB Simulink setting.

INTRODUCTION

The current power system uses centralized control, and the load prediction is mostly utilized to guide energy generation. As more and more renewable energy sources (RESs) are produced and introduced into the electricity system, RES interference is becoming a bigger stability issue.

The majority, however, are not compatible with future low-voltage RES panel systems, such as solar roof (PV) and small-power wind power plants, for example, because they are designed for high or moderate voltage applications. Voltage and/or power flow are regulated using adaptable alternating current transmission systems.

To counter this need, for future distributed microgrid systems, electrical spring (ES) technology has been proposed to pass line voltage fluctuation to the so-called non-critical loads (NCLs), i.e. loads tolerating wide voltage range, to preserve the voltage adjusted over so-called critical loads (CLs), i.e. the loads that tolerate limited voltage range supplies. The switch takes place through an automated load- balance with ES power generation. The ES and NCL collection are the so-called intelligent load. The voltage through CLs is hereafter referenced as grid voltage and the parallel SL.

To date, a number of documents on ES topologies and their management strategies have been released. The first version (ES-1), however, only allows reactive power to be controlled, and the second version (ES-2), as the DC condenser in ES can be replaced by a battery-like voltage source. The latest ES type without NCL is the third version (ES- 3). The so-called fourth version (ES-4) dramatically alters the output of the ES since it causes the NCL voltage to adjust the same way as the line voltage when an additional transformer is inserted into the initial ES-2. Various ES-2 control schemes have been documented in past work. For example, the input current can be regulated by the use of the dq0 transformation. However, this solution cannot preserve the grid voltage in an open-loop mode unchanged.

Even when the grid voltage is changed with a closed-loop with the PI-regulator, the power factor adjustment is the key concern rather than voltage control. In the case of Ś power, the device modeling that uses circuitry parameters is proposed to change instantaneous phase of CL voltage. The RCD control has recently been

developed to isolate the power angle of the SL from the voltage over the CL, making ES-2 ready for incorporation into many systems, such as water heaters. It still has some drawbacks, however. In the case of an NCL-variable or non- linear NCL, for instance, the power angle should be known in advance. Moreover, reactive power compensation by ES is difficult to obtain.

In this paper, power control of ES-2 is evaluated for a realistic application. Consider the example of a low-power outdoor wind power plant The MPPT technique is usually used in wind or solar generating power stations.

The electric loads in households, both of CL and NCL, consume tracked, active power. The active and reactive power produced by the plant is calculated by ES at the same position as the wind turbine, even if it changes rapidly. This helps ES to handle the input power both active and reactive in such a situation and enables the RMS value of the CL voltage to be regulated at the pre-set value by the latter control. For example, the control system cannot regulate the active power regardless of the reactive power. While the β control can achieve constant active power compensation, its limitations can still not be overcome.

The control RCD can instead adjust the grid voltage and, with separate radial and choral behavior, can also adjust the SL power factor. But the condition in which active input power is constant is not discussed. Even if one can demonstrate that RCD controls can address such a situation, the reactive power calculations required for ES, particularly in transients, are highly involved. This paper aims at the huge applications of ES-2 in distributed power systems. As a solution of the limitations of current control methods, this paper proposes simple active and sensitive power controls. The control proposed not only disconnects active and reactive power, but also depends on local signal manipulation, without knowledge about the ES-2 circuit parameters, voltage of the line, and parameters. In addition to simulations, trials to check the power management capabilities of the ES-2 implementing the proposed control are performed in three phases.

ELECTRIC SPRING

EXISTING SYSTEM

ESTopology There are two types of electrical loads, CLs and NCLs. ES is an electrical system that can pre-set the CL voltage to NCL when passing voltage fluctuations from the sources. Figure.1. ES-2 consists of a single-phase voltage source inverter (VSI), an L philter and a condenser with a voltage of up to NCL that is surrounded by the dotted line. In addition, CL is Z2, NCL is Z3, the line voltage VG is RESs, and the line resistance and induction are R1 and L1. CL and SL are supplied by the branch with Viand the line impedance. VS denote the common point (PCC) tension that is the CL tension as well.

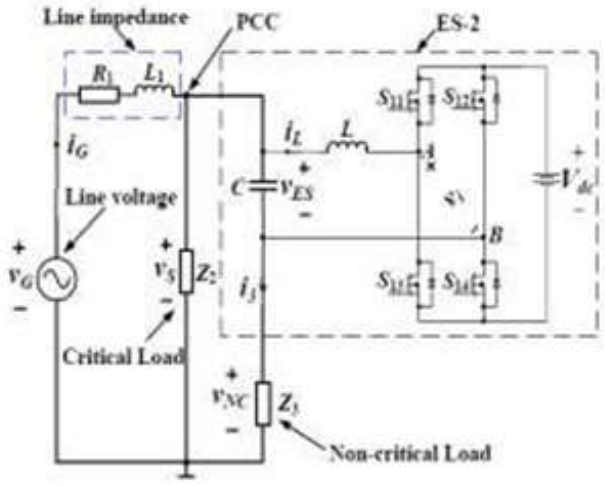

Fig1.Topology of ES-2 and associated circuitryPower Control of Existing ES-2

Control is one of ES-2's power control methods and involves a double loop monitor, as shown in fig.2 (a). The

external loop is shut down by the PR controller around the CL voltage while the inner loop is shut down by the P controller around theES current.

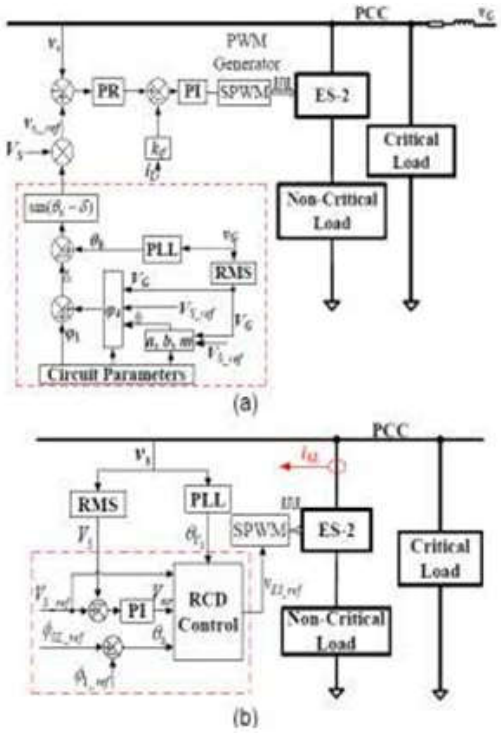

Fig 2.ES-2 control diagrams for (a) δ control, (b) RCD control.

The Control is intended to set the immediate step for the PR regulator of the reference voltage. The ¨ calculation method is based on an interpretation of the vector and ensures ES works in constant active input mode. The control objectives of ES-2 are achieved once the CL voltage is regulated. The β measurement, performed on the blocks found in theshattered line of Fig.2 (a), is the key to the operation and, thus, to the realization of control objectives. Theμ measurement is based on the ES-2 topology modelas shown in Figure 2 and uses circuit parameters, thus affecting their varying accuracy of control. In addition, since the co control is a vector-based phasecontrol, the Vc RMS value (marked as VG) isrequired to measure the angle μ. Therefore, VGshould be identified beforehand.

To detect VG, communication technology is needed between two nearby ESs because of the transmission line between the ES -2 and the grid . VGis far from ES -2. The cost of applying ¨control to ES - 2 is caused by this disadvantage.

In Fig.2 (b) you can see the RCD control chart for ES-2. There is a decomposition of the ES voltage in two ways, namely radial and choral. The PCC voltage is controlled with the radial control by setting an apparent power consumed by SL, while thepower angle of SL is controlled by the choral control at the pre-set value. This role makes the SL intelligent, since ES-2 can regulate the apparent power and power angle from SL independently. From this point of view, the control by RCD is aimed at regulating the strength of the SL. Although it is not the same as go which requires nearly all of the circuitry parameters, the NCL impedance angle has to be known beforehand. ES-2 in reactive power compensation mode is also very difficult to run. Moreover, it is not clarified how to deal with the situation when active input power differs.

Requirements for the Proposed Power Control

- In addition to the above review, the following criteria should be developed for a new method of power control:

- There's no need to detect grid voltage information far removed from PCC, such as go regulation
- Need to distinguish the active input power control loop from that of the PCC voltage orreactive input power
- Easy to execute and lower than othercomputing burdens

PROPOSED SYSTEM

It is presented the proposed power control and describes its ability through local signal manipulationto achieve a quick, active and reactive ES-2 power control. The single-phase derogating system is adopted in the proposed control.

ES system's active and reactive capacity

The vs. (t) and current i1 (t) sinusoidal voltage can beexpressed

$$v_S(t) = \sqrt{2}V_S \cos(\omega t + \phi) \quad (1)$$

$$i_1(t) = \sqrt{2}I_1 \cos(\omega t + \psi) \quad (2)$$

Whilst ± and go are the initials, go is angular, the values vs. (t) and i1 (t), respectively, are indicated by vs. (t) and i1 (t) rms.

By looking at active, reactive and apparent power from the PCC on the right side in Fig.2 you can express the active, reactive and apparent power from (3) to (5), which are the total active and reactivepower absorbed by the ES, the CL and the NCLtogether, in particular.

$$\begin{aligned} \tilde{S} &= \vec{V}_S \cdot \vec{I}_1^* \\ &= V_S I_1[\cos(\phi - \psi) + j\sin(\phi - \psi)] \\ &= P_{in} + jQ_{in} \end{aligned} \quad (3)$$

$$P_{in} = V_S I_1 \cos(\phi - \psi) \quad (4)$$

$$Q_{in} = V_S I_1 \sin(\phi - \psi) \quad (5)$$

The active and reactive power on a rotating frame canbe expressed by the variables

$$P_{in} = v_d i_d + v_q i_q \quad (6)$$

$$Q_{in} = v_q i_d - v_d i_q \quad (7)$$

The vein components of the derogating structure wherevdand vqare. I d and is the same comparison.

(6) And (7) can then be re-written when the vector ofvises is aligned along the d-axis of the rotating frame

$$P_{in} = v_d i_d \quad (8)$$

$$Q_{in} = -v_d i_q \quad (9)$$

It should be remembered that the minus sign of the power control loops is used in terms of (6) to (9). The polarities of Pin and Qin can be seen from (8) and(9). Infers should be inserted on the lower side and Pinero on the plus side. However, a path opposite to that of the grid connected converter (GCC) is chosen to show input current in Fig2. (A). the positions and the related references of the active and reactive forces are thus exchanged in Fig.2 (a). This is because the current direction in Fig.7.2. (a) Is picked.

Fig.2. (b) provides a thorough measurement of Pin and Qin whereby the Fourier Transformation is used to derive peak and phase angles from the quantity of viand i1 that has been detected. The diagram of Fig.2.

(b) Can easily be recognized by (4) and (5).

The vector matrix from the stationary frame of αβ to the rotating system and its reverse is expressed in the following terms

$$T(\hat{\theta}) = \begin{bmatrix} \cos\hat{\theta} & \sin\hat{\theta} \\ -\sin\hat{\theta} & \cos\hat{\theta} \end{bmatrix} \quad (10)$$

$$T(\hat{\theta})^{-1} = \begin{bmatrix} \cos\hat{\theta} & -\sin\hat{\theta} \\ \sin\hat{\theta} & \cos\hat{\theta} \end{bmatrix} \quad (11)$$

Where a closed loop (PLL) block is detected in the instantaneous step of PCC voltage.

Power Control of ES-2

The control diagram of the basic power control proposed is illustrated in the Fig block. 3. (A) the dotted line is used. This control requires that variables like input current i1 and CL voltage vs. are detected. The active and reactive input power of the ES system is marked

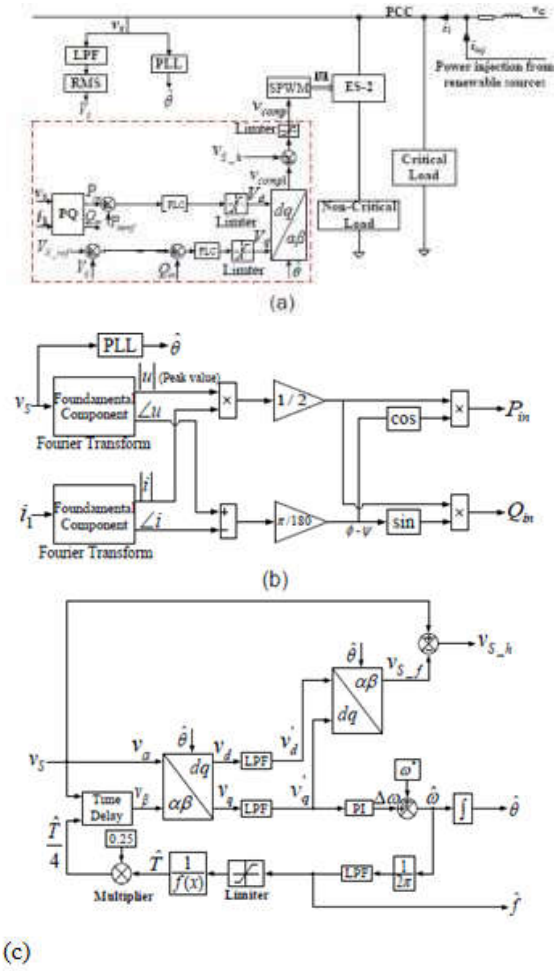

Fig 3. The proposed power control of ES-2. (a) Control diagram. (b) Calculation diagram ofactive and reactive power. (c) Functions of PLL and harmonic extraction.

Like Pin and Qin, the instantaneous values of viand i1 as demonstrated by the scheme of Fig. 3(b), which already includes the Matlab / Simulink function block, are manipulated.

RMS and the instantaneous CL voltage step are, as per Fig.3. (A)Detected by the blocks RMS and PLL. Separate FUZZY controls regulate the powers Pinand Qin. In particular, the d-axis regulator controls pin and Qin are governed by one in the q-axis. If the control target is the CL voltage rather than Qin, the external loop of the q axis with a FUZZY control unitis added closed, and the output reflects the Qin relation, called Infer.

For the vcomp1 modulation signal the output signals from the FUZZY controller are processed in bothcircuits via the inverse dq-to-αβ transformation. It is worth noting that the harmonic deletion functionality is introduced by deleting the harmonic variable known as vS h from the vcomp1 in Fig. 3. (A). The SPWM technique, after a

limiter, produces drive signals for the VSI transistors.

PLL single stage single step

In the calculation of phase, A and the angular frequency A and vs., the standard Synchronous Reference Frame PLL (SRF-PLL) is used. Detailed diagram of the SRF-PLL is in fig. 7.2. (c) WhereIV and IV are marked as "alternate" and "aligned" respectively. Fig. 3. (c). and that's what 100′ is all about.

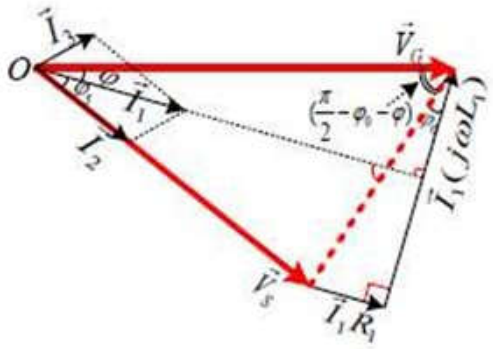

Fig 4. Vector diagram of ES-2 circuit withresistive CL.

Operating Limitations

It is thought that ES-2 will automaticallyregulate active input and CL voltage. But within suchconstraints, this is possible. The diagram for the vector in Fig. 4 is a good example by setting a resistive CL to further illustrate. The input vectors, CL and NCL streams and CL-voltages are shown in Fig.4 I1, I2, I3, VG, VS respectively. The all is determined by the angle of the stage I1 is the VG, theangle of the phase I2 is the I1 and the angle of the line impedance is the ±5. The angle of the phaseangle is the from (3) to (5) it is deduced that once the VG is set, the constant value of Grid implies that I 1 COS¨is constant as well. It follows from Fig.4

$$\sin(\varphi+\varphi_3)=\frac{P_{grid}}{V_G V_S}\frac{\cos(\varphi+\varphi_0)}{\cos\varphi}\sqrt{R_1^2+(\omega L_1)^2} \quad (12)$$

The amplitude of the sin function is not greater than 1. Then, from (12), one gets

$$P_{grid}\le\left|\frac{V_G V_S}{\sqrt{R_1^2+(\omega L_1)^2}}\frac{\cos\varphi}{\cos(\varphi+\varphi_0)}\right| \quad (13)$$

Considering that 0 is much less than ·, and the cosine terms in (13), it follows from this that the line impedance of microgrid is inductive. The overall Grid can therefore be calculated as

$$P_{grid}\le\frac{V_G V_S}{\sqrt{R_1^2+(\omega L_1)^2}} \quad (14)$$

Grid includes the transmission line losses, which means the Pin is smaller than Grid.

SIMULATION RESULTS

CASE A: Input Active Power Variation

In this part, three different values are selected for VG to monitor its behavior when Pinrefvaries. Figures 5, 6, 7 shows the simulation results when Pinrefvaries. In each subfigure, four channels are recorded, reporting vG, Pinref, Pin and RMS value of the CL voltage, respectively.

Results in a full-time range are also shown in Fig. 5, in which Pinrefis changed from 1.6kW to 1.1kW at 6s and then back to 1.6kW at 12s. It is observed that Pin tracks Pinrefwell while VS is regulated to 220V as Pinrefvaries. To validate the proposed control further, the values of Pinrefare raised and simulated, as shown in

Fig.6. The waveforms confirm that the control objectives are also realized at high powerratings. To demonstrate how the control operates with the ES-2 power quantities, they are traced in Fig.6, setting VG=200 as an example. In each subfigure, four channels are recorded, reporting Pin, PCL, PES and PNCL against their pre-set values. Thefour power quantities represent the input active power, and the active powers absorbed respectively by the CL, the ES-2, and the NCL. In the first channel of each subfigure, PinrefandPin are traced with the dashed and solid lines, respectively. In Fig.

7, Pinrefis set to 8kW from 0 to 6s, then to 4kW from6s to 12s and then to 2kW from 12 to 20s.

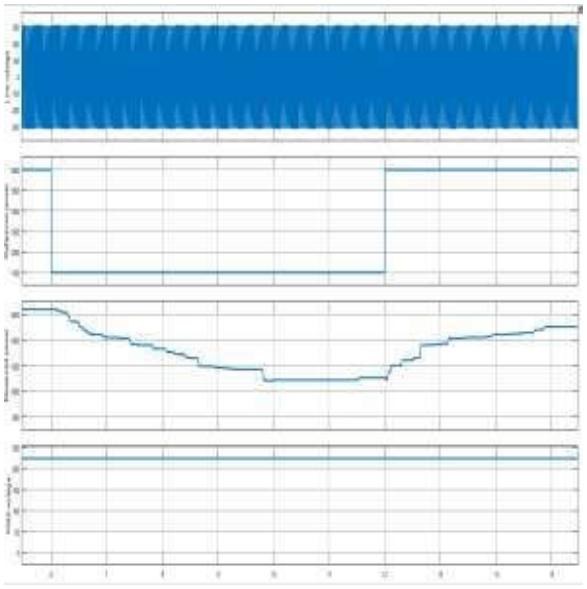

Fig 5. Simulation waveforms under differentvariations of the input active power From 1.6kW to 1.1kW and then back to 1.6kW

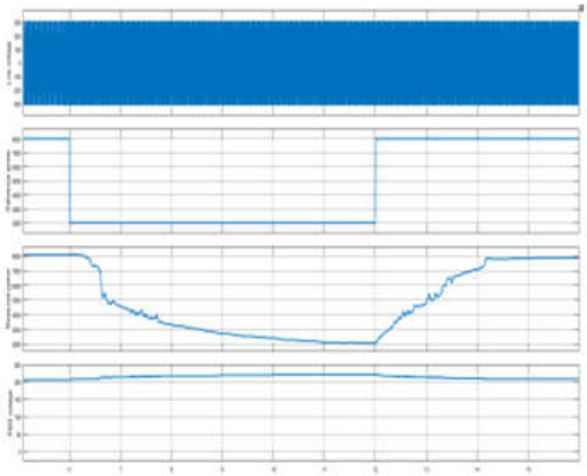

Fig 6. Simulation waveforms under different variations of the input active power from 8kW to 2kW and then back to 8Kw

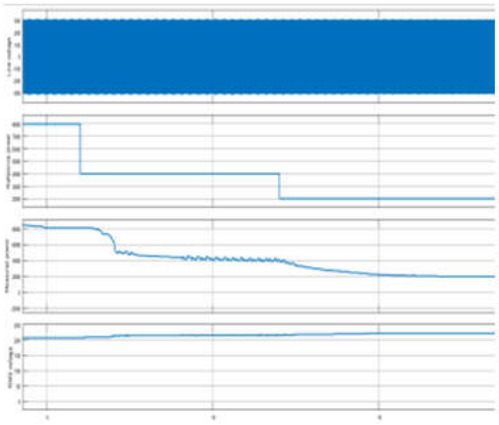

Fig 7. Simulation waveforms under differentvariations of the input active power from 8kW to 4kW and then to 2kW

CASE B: Line Voltage Variation

In this Subsection, the ES-2 transient responses to a change of VG are monitored with Pinreffixed. They are traced in Figs.8 and 9. In each subfigure, four channels are recorded, reporting line voltage, reference value of the input active power, input activepower and RMS value of CL voltage, respectively. InFig. 8, VG is changed between two different values, more specifically it is equal to 240V from 0 to 6s; afterwards it jumps to 210V at 6s and remains at this value up to 12s. The change of VG in Fig. 9 is the opposite of that in Fig.8. In both the simulations, Pinrefis set to 1.5kW and Pin remains at the pre-set value very accurately. Meanwhile, the RMS value of the CL voltage is regulated to 220V as required

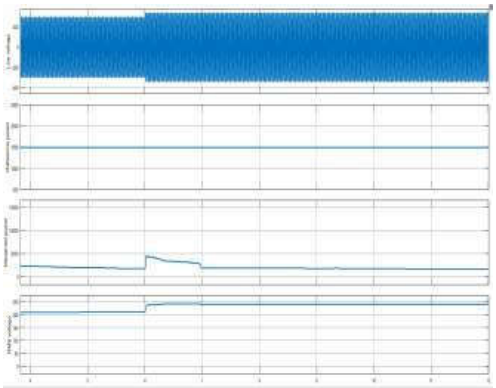

Fig 8. ES-2 responses to a change of the line voltage with Pinref=1.5kW. (a) From 240V to 210V

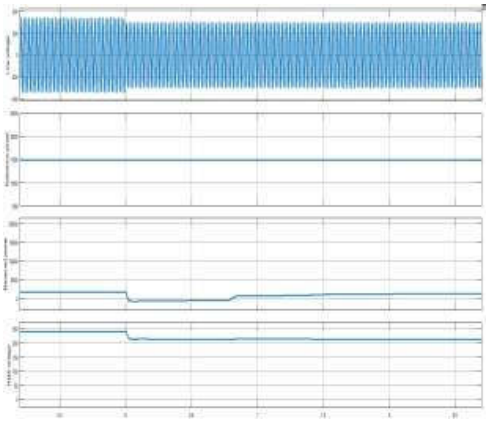

Fig 9. ES-2 responses to a change of the line voltage with Pinref=1.5kW. (a) From 210V to 240V

CASEC: Simulation waveforms before and after grid distortion.

a) Results of PLL

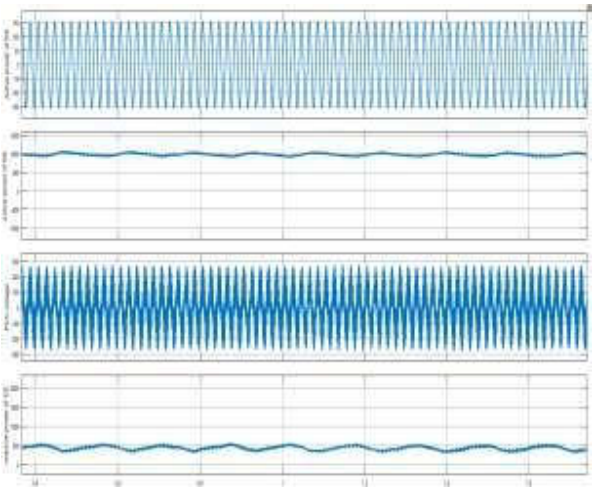

(a) Results of active power of ES system.

WITH FUZZY CONTROLLER

Simulation waveforms before and after grid distortion

(a) Results of PLL.

(b) Results power of ES system

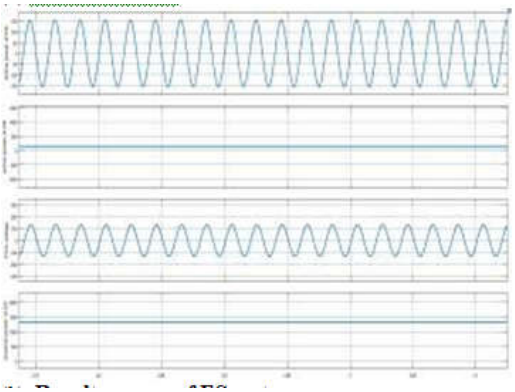

CONCLUSION

For the practical implementation of ES-2 in this text, the input active and reactive power control is proposed. The current control methods, such as Ścontrol and RCD control, have been evaluated and analyzed in general to establish that input active power and reagent power are the essences of the controls on ES-2. The ES-2 can handle the fluctuated power and ensure that it is fitted with the RES distributed generation, meaning the ES-2 can deal with the power captured by the MPPT algorithm. The efficacy of the proposed fuzzy control was validated via steady and transient analysis and also through grid anomalies the proposed fuzzy control was validated by simulation results.

REFERENCES

1. M. Cheng and Y. Zhu, ―The state of the art of wind energy conversion systems and technologies: Are view,‖ Energy Conversion and Management, vol.88, pp. 332–347, Dec. 2014.
2. P. Soothed and R. D. Miller, ―Design and implementation of an 11-level inverter with FACTS capability for distributed energy systems,‖ IEEE J. Emerging Sel. Topics Power Electron., vol.2, no. 1, pp. 87–96, Mar. 2014.
3. L. Wang, and D. N. Truong, ―Stability enhancement of a power system with a PMSG-based and a DFIG-based offshore wind farm using a SVC With an adaptive-network-based fuzzy inferencesystem,‖ IEEE Trans. Ind. Electron., vol. 60, no. 7, pp. 2799–2807, Jul. 2013.
4. Y. Zhang, X. Wu and X. Yuan, ―A simplified branch and bound approach for model predictive control of multilevel cascaded H-bridge STATCOM,‖ IEEE Trans. Ind. Electron., vol. 64, no. 10, pp. 7634–7644, Oct. 2017.
5. W. Wang, L. Yan, X. Zeng, B. Fan, and J. M. Guerrero, ―Principle and design of a single-phase inverter based grounding system for neutral-to-ground voltage compensation in distribution networks,‖ IEEE Trans. Ind. Electron., vol. 64, no. 2, pp. 1204–1213, Feb. 2017. Q. Sun, J. Zhou, J. M. Guerrero, and H. Zhang,
6. Hybrid three-phase/single-phase microgrid architecture with power management capabilities,‖ IEEE Trans. Power Electron., vol. 30, no. 10, pp. 5964–5977, Oct. 2015.
7. J. M. Guerrero, J. C. Vasquez, J. Matas, L. G. de Vicuna, and M. Castilla, ―Hierarchical control of droop-controlled AC and DC microgrids—a general approach toward standardization,‖ IEEE Trans. Ind. Electron., vol. 58, no. 1, pp. 158–172, Jan. 2011.
8. S. Y. R. Hui, C. K. Lee, and F. Wu, ―Electric springs—A new smart grid technology,‖ IEEE Trans. Smart Grid, vol. 3, no. 3, pp. 1552–1561, Sept. 2012.
9. S. C. Tan, C. K. Lee, and S. Y. R. Hui, ―General steady-state analysis and control principle of electric springs with active and reactive power compensations,‖ IEEE Trans. Power Electron., vol. 28, no. 8, pp. 3958–3969, Aug. 2013.
10. C. K. Lee and S. Y. R. Hui, ―Input AC voltage control bi-directional power converters,‖ U.S. Patent 13/907, 350, May 31, 2013.
11. Q. Wang, M. Cheng, G. Buja, and Z. Chen, ―A novel topology and its control of single-phase electric springs,‖ in Proc. Int. Conf. Renewable Energy Res. Appl., 2015, pp. 267–272.
12. Q. Wang, M. Cheng, and Y. Jiang, ―Harmonics suppression for critical loads using electric springs with current-source inverters,‖ IEEE J. Emerging Sel. Topics Power Electron., vol. 4, no. 4, pp. 1362–1369, Dec. 2016.
13. S. Yan, S. C. Tan, C. K. Lee, and S. Y. R. Hui,―Electric spring for power quality improvement,‖ in Proc. IEEE Appl. Power Electron. Conf. Expo., 2014,pp. 2140–2147.
14. Q. Wang, M. Cheng, Z. Chen, and Z. Wang,―Steady-state analysis of electric springs with a novel δ control,‖ IEEE Trans. Power Electron., vol. 30, no. 12, pp. 7159–7169, Dec. 2015.

15. K. T. Mok, S. C. Tan, and S. Y. R. Hui,–Decoupled power angle and voltage control of electric springs,‖ IEEE Trans. Power Electron., vol. 31, no. 2, pp. 1216–1229, Feb. 2016.
16. X. Chen, Y. Hou, S. C. Tan, C. K. Lee, and S. Y.R. Hui, –Mitigating voltage and frequency fluctuation in microgrids using electric springs,‖ IEEE Trans. Smart Grid, vol. 6, no. 2, pp. 508–515, Mar. 2015.
17. M. Andresen, G. Butichi, and M. Liserre,–Thermal stress analysis and MPPT optimization of photovoltaic systems,‖ IEEE Trans. Ind. Electron., vol. 63, no. 8, pp. 4889–4898, Aug. 2016.
18. F. Paz, and M. Ordonez, –High-performance solar MPPT using switching ripple identification based on a lock-in amplifier,‖ IEEE Trans. Ind. Electron., vol. 63, no. 6, pp. 3595–3604, Jun. 2016.
19. J. A. Munoz, J. R. Espinoza, C. R. Baier, L. A. Moran, E. E. Espinosa, P. E. Melin, and D. G. Sbarbaro, –Design of a discrete-time linear control strategy for a multicell UPQC,‖ IEEE Trans. Ind. Electron., vol. 59, no. 10, pp. 3797–3807, Oct. 2012.
20. S. Golestan, and J. M. Guerrero, –Conventional synchronous reference frame phase-locked loop is an adaptive complex filter,‖ IEEE Trans. Ind. Electron., vol. 62, no. 3, pp. 1679–1682, Mar. 2015. of interest is FACTS.